On the X-ray low- and high-velocity outflows in AGNs

J.M. Ramírez [1][⋆] and F. Tombesi [2,3]

[1] *Leibniz-Institut für Astrophysik Potsdam, An der Sternwarte 16 D-14482 Potsdam, Germany*
[2] *Department of Astronomy and CRESST, University of Maryland, College Park, MD 20742, USA*
[3] *Laboratory for High Energy Astrophysics, NASA/Goddard Space Flight Center, Greenbelt, MD 20771, USA*

ABSTRACT

An exploration of the relationship between bolometric luminosity and outflow velocity, for two classes of X-ray outflows in a large sample of active galactic nuclei has been performed. We find that line radiation pressure could be one physical mechanism that might accelerate the gas we observe in warm absorber, $v \sim 100 - 1000$ km s^{-1}, and on comparable but less stringent grounds the ultra-fast outflows (UFOs), $v \sim 0.03 - 0.3c$. If comparable with the escape velocity of the system; the first is naturally located at distances of the dusty torus, ≈ 1 pc, and the second at sub-parsec scales, ≈ 0.01 pc, in accordance with large set of observational evidence existing in the literature. The presentation of this relationship might give us key clues for our understanding of the different physical mechanisms acting in the center of galaxies, the feedback process and its impact on the evolution of the host galaxy.

Key words: black hole physics - X-ray: galaxies - galaxies: active

1 INTRODUCTION

Mildly relativistic and non-relativistic absorption troughs are observed in the X-ray spectra of active galactic nuclei (AGNs). A qualitative separation is usually done between classical $v \sim 100 - 1000$ km s^{-1} warm absorbers, we refer to here (throughout paper) as *low-velocity* outflows (Blustin et al. 2005; McKernan et al. 2007), and ultra-fast outflows (UFOs) $v > 10,000$ km s^{-1}, we refer to here as *high-velocity* outflows (Tombesi et al. 2010a,b).

On one hand, the extracted velocity from the classical $v \sim 100 - 1000$ km s^{-1} warm absorber is mainly obtained using the Fe M-shell $2p - 3d$ unresolved transition array (UTA) (Behar et al. 2001; Ramírez et al. 2008), and O VII or O VIII resonance lines (e.g., George et al. 1998, the hallmark of the classical warm absorber). The spatial location of this absorbing material is uncertain. Models of X-ray absorbers in AGN place them at a wide range of distances from the central source. Specifically they are suggested to be winds originating from the accretion disk (Murray et al. 1995; Elvis 2000), located at the dusty (~ 1 pc) torus scales (Krolik & Kriss 2001) or even beyond the narrow-line region (e.g. Ogle et al. 2000).

On the other hand, blueshifted Fe K absorption lines have been detected in recent years at $E > 7$ keV in the X-ray spectra of several radio-quiet AGNs (e.g., Chartas et al. 2002, 2003; Pounds et al. 2003; Dadina et al. 2005; Markowitz et al. 2006; Braito et al. 2007; Ramírez

2008; Cappi et al. 2009; Reeves et al. 2009; Tombesi et al. 2010a,b). They are usually interpreted as due to resonant absorption from Fe XXV-XXVI associated with a zone of circumnuclear gas photoionized by the central X-ray source, with ionization parameter $\log \xi \sim 3 - 6$ erg/s cm and column density $N_H \sim 10^{22} - 10^{24}$ cm^{-2}. The energies of these absorption lines are systematically blueshifted and the corresponding velocities can reach up to mildly relativistic values of $\sim 0.03c - 0.3c$. These findings are important because they suggest the presence of previously unknown massive and highly ionized absorbing material outflowing from their nuclei, possibly connected with accretion disk winds/ejecta (e.g., King & Pounds 2003; Proga & Kallman 2004; Sim et al. 2008; Ohsuga et al. 2009; King 2010b; Sim et al. 2010).

Several acceleration mechanisms have been proposed to explain these outflows: (1) thermally accelerated winds (Krolik & Kriss 2001); (2) radiation pressure through Thomson scattering and magnetic forces (MHD, Ohsuga et al. 2009); (3) and radiation pressure due to the absorption of spectral lines (e.g., Proga & Kallman 2004; Ramírez 2008; Schurch et al. 2009; Sim et al. 2010; Ramírez 2011). Although the first one can explain the velocities we observe in the low-velocity outflows, it can be excluded because it can not explain the $\sim 0.1 - 0.2c$ we observe in UFOs (Tombesi et al. 2010a,b). Ohsuga et al. (2009) seem to reproduce the velocities observed in *low-* and *high-velocity* outflows. On the other hand, Arav et al. (1994); Ramírez (2008); Saez et al. (2009); Chartas et al. (2009), invoke radiation pressure due to lines to explain the $\sim 0.2c$ outflow

[⋆] E-mail:jramirez@aip.de

detected in a good S/N X-ray spectrum of a *high-z* quasar (the broad absorption line [BAL], APM 08279+5255), and they reproduce, as part of the procedure, the Fe XXV-XXVI lines detected at $E > 7$ keV. Here we focus on this kind of approach, since it allows us to explore, very efficiently, a wide range of physical parameters of the system.

The goal of this Letter is to place a proof of idea for a systematic study about the operating acceleration mechanisms in both; X-ray *low-* and *high-velocity* outflows, using an anisotropic radiative pressure framework (e.g., Proga et al. 2000; Proga & Kallman 2004; Liu & Zhang 2011), beginning with line radiation pressure.

We present the observables from which we build the model in §2. The details of the proposed model are presented in §3. The results and the discussion are in §4. We summarize in §5.

2   OBSERVABLES

In this section we present the observables of the two types of outflows, since they are the initial motivation for the proposed model.

2.1   The low-velocity outflows

When describing the physical conditions of warm absorbers, it is common to use the definition of ionization parameter $\xi = \frac{4\pi F_{\rm ion}}{n_H}$ (Tarter et al. 1969), where $F_{\rm ion}$ is the total ionizing flux ($F_{\rm ion} = L_{\rm ion}/4\pi r^2$), and n_H is the gas density. The source spectrum is described by the spectral (specific, energy dependent ϵ) luminosity $L_\epsilon = L_{\rm ion} f_\epsilon$, where $L_{\rm ion}$ is the integrated luminosity from 1 to 1000 Ryd, and $\int_1^{1000 \ {\rm Ryd}} f_\epsilon d\epsilon = 1$.

So we describe the ~ 1000 km s^{-1} warm absorber outflows as absorbing material around a supermassive black hole (SMBH) with mass $M_{BH} \sim 3 \times 10^7$ (Peterson et al. 2004; Blustin et al. 2005), column density of the absorbing material $N_H \sim 10^{20} - 10^{22}$ cm^{-2}, flowing outwards at velocities $v \sim 100 - 2000$ km s^{-1}(e.g., Kaspi et al. 2002; Krongold et al. 2003, 2005; Ramírez et al. 2005), at medium ionization states $\log \xi \sim 0 - 3$ erg s^{-1} cm (Blustin et al. 2005).

When computing the energetics they find mass loss rates of [1] $\dot{M}_{out} \approx 0.6$ M$_\odot$ yr^{-1} ratios of $\dot{M}_{out}$ to accretion rates [2], $\dot{M}_{out}/\dot{M}_{acc} \approx 5$ and kinetic luminosity [3] $L_{EK} = \frac{\dot{M}_{out}v^2}{2}$, of the orders of $10^{38} - 10^{41}$ erg/s, representing less than 1 % of the bolometric luminosity (Blustin et al. 2005). The main conclusion from these estimations is that these outflows contributes little to the energy injected in to the host galaxy. But the amount of matter processed over the AGN lifetime can be significant (also in accordance with Krongold et al. 2007, for instance).

2.2   The high-velocity outflows

The characteristics of the ultra-fast outflows with $v \geqslant$10,000 km s^{-1} ($\geqslant$0.03c) can be derived from the blue-shifted Fe XXV-XXVI absorption lines detected by Tombesi et al. (2010b) in a complete sample of local Seyfert galaxies. Such features are detected in $\sim$40–60% of the sources, which suggests a covering fraction of $C\sim$0.5. Tombesi et al. (2011) also performed a photo-ionization modeling of these lines. They derived the distribution of the outflow velocities, which ranges from $\sim$0.03c up to mildly relativistic values of $\sim$0.3c, with a peak and mean value at $\sim$0.14c. As expected, these absorbers are highly ionized, with $\log\xi\sim$3–6 erg s^{-1} cm, and have large column densities, in the range $N_H\sim$10^{22}–10^{24} cm^{-2}.

The SMBH masses of the Seyferts in the Tombesi et al. (2010b) sample have a mean value of $M_{BH} = 5.3 \times 10^7$ $M_\odot$ (Marchesini et al. 2004; Peterson et al. 2004).

When computing the energetics of these outflows, we see that these are more massive than the low-velocity ones, $\dot{M}_{out}\sim 0.1 - 1$ M$_\odot$ yr^{-1} $\sim\dot{M}_{acc}$, and also much more powerful, with a mechanical power of $\sim$10^{43}–10^{45} erg/s (e.g., Pounds et al. 2003; Markowitz et al. 2006; Braito et al. 2007; Cappi et al. 2009; Tombesi et al. 2010b). The latter value is $\sim 5 - 10\%$ of the bolometric luminosity. Therefore, the high-velocity outflows may potentially play an important role on the expected cosmological feedback from AGNs (e.g., King 2010a,b).

3   THE MODEL

We build our model based on observational evidence, basically from two sources: Blustin et al. (2005) for the classical $v \sim 100 - 1000$ km s^{-1} warm absorbers, referred here as *low-velocity* outflows, and Tombesi et al. (2010b) for the ultra-fast outflows (UFOs) $v \geqslant 10,000$ km s^{-1}, referred here as *high-velocity* outflows.

As we see, together the two classes of outflows cover a wide range in velocity and black hole masses. We seek a physical model which provides the context to explain (to first approximation), part of the observational evidence we have up to now.

In order to do that, and to gain some insight into the relationship between outflow velocity (v_{out}) and luminosity, we invoke the velocity profile as a function of radius, given by hydrodynamical calculations (Proga et al. 2000). The mathematical shape of the relation is given by assuming an outflow accelerated by radiation pressure from a central source with a bolometric luminosity L_{bol}, and a mass of M_{BH}:

$$v_{out}[i] = \left[2GM_{BH}[i] \left(\Gamma_f \frac{L_{bol}[i]}{L_{Edd}[i]} - 1 \right) \left(\frac{1}{R_{in}} - \frac{1}{R} \right) \right]^{1/2}, (1)$$

where L_{Edd} is the Eddington luminosity, Γ_f is the force multiplier, where the acceleration due to the absorption of discrete lines is encapsulated (Laor & Brandt 2002), R_{in} is the radius at which the wind is launched from the disk, and R is the distance of the accelerated portion of the outflow from the central source. The index i, runs simultaneously over the two distributions: velocity/BH mass. Assuming that we observe the gas when it has reached the terminal velocity of the wind, i.e. v_{out} at $R = \infty$, we can write:

---

[1] Mean of the $\dot{M}_{out}$ reported by Blustin et al. (2005) in their Table 4, excluding Ark 564 (outlier $\dot{M}_{out} = 23$ M$_\odot$ yr^{-1}).
[2] Mean of the $\dot{M}_{out}/\dot{M}_{acc}$ reported by Blustin et al. (2005) in their Table 4, excluding Ark 564 (outlier $\dot{M}_{out}/\dot{M}_{acc} = 550$).
[3] Excluding PG 0844+349 and PG 1211+143.

$$L_{bol}[i] = \frac{L_{Edd}[i]}{\Gamma_f} \left(\frac{v_{out}[i]^2 R_{in}}{2GM_{BH}[i]} + 1 \right). \tag{2}$$

Now we have the basic ingredient of the model, and we are ready to build our two classes of outflows.

SET 1: *High-velocity.* This synthetic sample is composed from 1000 black holes with masses normally distributed with mean, $\mu_m = 2.6 \times 10^7$ M$_\odot$ and standard deviation, $\sigma_m = 1.3 \times 10^7$ M$_\odot$ [4]. Also we use a normal distribution for the outflow velocity of the absorbing gas around the BH with $\mu_v = 57,000$ km s^{-1} (this is the best-fit value for SET 1), and $\sigma_v = 15,000$ km s^{-1}.

SET 2: *Low-velocity.* In this case we use 1000 black holes with masses normally distributed with the same mean, $\mu_m = 2.6 \times 10^7$ M$_\odot$ and standard deviation, $\sigma_m = 1.3 \times 10^7$ M$_\odot$ as before but we use a normal distribution for the outflow velocity of the absorbing gas around the BH with $\mu_v = 1800$ km s^{-1} (this is the best-fit value for SET 2), and $\sigma_v = 600$ km s^{-1}.

The best-fit values of $\mu_v(1)$ and $\mu_v(2)$ (as well $\Gamma_f(1) = 250$ and $\Gamma_f(2) = 40$, see next section), are estimated by comparing a grid of models computed using $10,000 \leqslant \mu_v(1) \leqslant 70,000$ (km s^{-1}) and $100 \leqslant \mu_v(2) \leqslant 2000$ (km s^{-1}), with the corresponding set of observation: SET 3 *vs* Tombesi et al. (2011) and SET 4 *vs* Blustin et al. (2005). We performed the comparison using a Kolmogorov-Smirnov test. We take the $\mu_v(1)$ and $\mu_v(2)$ (as well $\Gamma_f(1) = 250$ and $\Gamma_f(2) = 40$, see next section) which give maximum p-values of the test. The final p-value for the comparison SET 3 *vs* Tombesi et al. (2011) gives ≈ 0.8 ($D = 0.16$) and for the SET 4 *vs* Blustin et al. (2005) ≈ 0.07 ($D = 0.38$).

The launching radius R_{in}, for each set of simulations is based on the results of Blustin et al. (2005) for SET 2; i.e., $R_{in}(set\ 2) = 1\ pc$ (orders of magnitude value). For SET 1, we set $R_{in}(set\ 1) = 0.01\ pc$, based on Tombesi et al. (2010a,b).

4 RESULTS AND DISCUSSION

In this section we discuss the results of our simulated samples and summarize their physical context and implications.

Figure 1 shows the theoretical relationship between outflow velocity and bolometric luminosity.

The curvature we see in v_{out} of SET 2 (and also SET 1, filled circles, our line of sight is along the flow, see below), is due to the quadratic dependence of the luminosity with v_{out} given by equation 2. It is worth noticing that if we assume a force multiplier of $\Gamma_f = 40$ (this is the best-fit value for SET 2 and SET 4, see section 3) ; we are able to reproduce the range of luminosities seen in Figure 4 of Blustin et al. (2005).

On the other hand this model is not reproducing well the dispersion we observe in Figure (4) of Blustin et al. (2005), which could be explained by the fact that equation 2 will give radially accelerated flows, or in other words, that
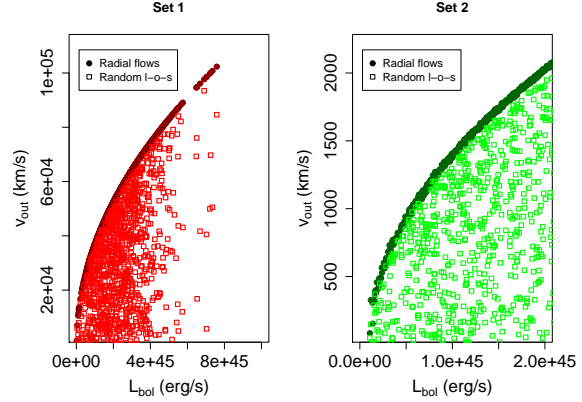
Figure 1. Velocity of the outflow *vs* the bolometric luminosity needed to accelerate the wind. Filled circles are the velocities observed if we see the wind along the flow. Open squares are including the effects of random line-of-sights (see text for discussion).

we are observing all the objects radially along the flow. To include the effect of observing random line-of-sights transversely through different sections of the flow we connect the observed velocity v_{obs} with the intrinsic radial velocity, i.e. $v_{obs} = v_{out}\cos\theta$, where θ is the angle between the outflow direction and the line of sight. Then using the same luminosities produced by SET 2, but plotting (open squares) against 1000 v_{obs}(s) randomly computed using a random generator of numbers (with $\pi/12 \leqslant \theta \leqslant \pi/2$) [5], and equation 2 with $v_{obs} = v_{out}\cos\theta$, we produce the sub-sample SET 4. It is easy to see that SET 4, resembles better the plot shown in Figure 4 of Blustin et al. (2005), taking into account the possible incompleteness of the sample.

Doing the same for the UFOs, we use the luminosities produced by SET 1 ($\Gamma_f = 250$, this is the best-fit value for SET 1 and SET 3, see section 3) but plotting (open squares) against 1000 v_{obs}(s) randomly computed using a random generator of numbers (with $\pi/12 \leqslant \theta \leqslant \pi/2$), and equation 2 with $v_{obs} = v_{out}\cos\theta$, to produce the sub-sample SET 3. In this case SET 3, better resembles the relationship between v_{out} and luminosity (see Figure 2).

In Figure 2 we place both classes of outflows together along with observational points taken from two samples of objects: 14 points out of the 23 objects reported by Blustin et al. (2005) (the others either did not report outflow velocity or were unknown), in the right panel; and 19 points from the sample of 19 objects were UFOs have been detected by Tombesi et al. (2011), in the left panel.

There are several interesting facts about the plot: (1) *the observational points* cover ≈ 3.8 orders of magnitude in velocity; (2) they cover ≈ 3 orders of magnitude in bolometric luminosity (from $\sim 10^{43} - 10^{46}$ erg/s); and (3) that our proposed model is able to reproduce most of the low-velocity points (11/14) (two of the points might fall in the high-velocity set instead) and, less stringently, half of the points for the high-velocity set (11/19), using one physical acceleration mechanism and three free parameters: mass

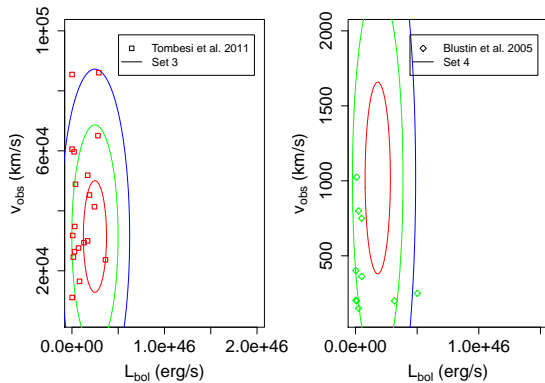**Figure 2.** Theoretical *vs* observational outflow velocity against luminosity. Ellipses (1,2 and 3 σ contours of the model) are theoretical calculations coming from two samples of outflows; *Left panel:* high-velocity (SET 3, i.e., including the effects of random line-of-sights), and *Right panel:* low-velocity (SET 4, i.e., including the effects of random line-of-sights). Open squares are observational points from the XMM-Newton radio-quiet sample of Tombesi et al. (2011), for the UFOs. The open diamonds are points compiled by Blustin et al. (2005).

of the BH (M_{BH}), outflow velocity (v_{out}) and force multiplier (Γ_f). On the other hand, there are two sectors where the deviations between model and theory are large: (1) the high-velocity/low luminosity; and (2) the low-velocity/high luminosity, both requiring a closer inspection to the completeness of the samples, and/or the addition of other acceleration mechanisms, like magnetic thrust for instance. But, this may be the topic of future work.

4.1   Anisotropic radiation pressure picture

We propose here that the low- and high-velocity outflows can be accelerated by the same physical mechanism (as is suggested by Figure 2); i.e., radiation pressure, and that the differences depend on the values of the 3 fundamental parameters: mass of the BH (M_{BH}), the object luminosity (L_{bol}) and force multiplier (Γ_f). *The values of Γ_f we have used are of the orders of those found in observational (e.g., Laor & Brandt 2002) and theoretical (e.g., Saez et al. 2011) works.* However, detailed photoionization computations are required to verify if the opacity of the gas under the physical conditions presented here can overcome the over-ionization problem (Proga et al. 2000), and are left for future work.

The anisotropic property of the radiation is basically demanded by the existence of obscured and un-obscured (Type 1 and Type 2) AGNs (Antonucci 1993), and it explains the decreasing of Type 2 AGNs as a function of the X-ray Luminosity (Hasinger 2008). It is also intrinsically linked to the existence of the dusty torus [6] and it gives the natural frame to locate our two classes of outflows. If comparable with the escape velocity of the system (a black hole of $M_{BH} = 5.3 \times 10^7$ M$_\odot$), fast-outflow, $v_{out} \sim 0.10c$, locates

escape radius at $r \sim (20 - 100)r_S$ (Schwarzschild radius, $r_S = \frac{2GM_{BH}}{c^2}$). This is very close to the SMBH, and the origin is likely the accretion disk.

Again, using $500 - 1500$ km s^{-1}, as escape velocity from a 2.6×10^7 $M_\odot$ BH, locates the gas at $\sim 0.1 - 1$ pc, well beyond the event horizon of the BH, and the broad line region (BLR; Laor & Draine 1993) as well, where the dusty torus is thought to be located.

5   SUMMARY

For the first time, an exploration on the relationship between bolometric luminosity and outflow velocity, for two classes of X-ray outflows in a large sample of active galactic nuclei has been performed. We find that: (1) Line radiation pressure is an efficient [7] mechanism to accelerate the low-velocity ($500 - 2000$ km s^{-1}) gas we observe in the classical ~ 1000 km s^{-1} warm absorber. (2) It might also become efficient to accelerate the high-velocity ($0.05 - 0.3c$) gas we observe in the UFOs. (3) They both might be placed in the same context of anisotropic radiation pressure (e.g., Proga et al. 2000; Proga & Kallman 2004; Liu & Zhang 2011).

However, there are many open questions, which will require close investigation and detailed modeling. In the first place the fact that we are assigning one type of outflow to different portions of the parameter space (M_{BH}, L_{bol} and Γ_f), does not preclude the existence of both in the same object. Also, careful studies of the connection between these outflows observed in X-rays and outflows seen in other bands of the electromagnetic spectrum, UV, infrared or optical (multi-wavelength studies) are important points to be addressed. Finally the close inspection of the main parameters of the system (M_{BH}, v_{out} and Γ_f) with cosmological parameters (like redshift) is of high relevance, and might be the topic of future works.

REFERENCES

Antonucci R., 1993, ARAA, 31, 473
Arav N., Li Z., Begelman M. C., 1994, ApJ, 432, 62
Behar E., Sako M., Kahn S. M., 2001, ApJ, 563, 497

---

[6] A convenient definition is that of cool ($\sim$1000 K) optically and geometrically thick gas in approximate rotational and virial equilibrium at $\sim$1 pc (Krolik & Begelman 1988).

[7] Based on observed force multipler (Laor & Brandt 2002).

Blustin A. J., Page M. J., Fuerst S. V., Branduardi-Raymont G., Ashton C. E., 2005, A&A, 431, 111

Braito V., Reeves J. N., Dewangan G. C., George I., Griffiths R. E., Markowitz A., Nandra K., Porquet D., Ptak A., Turner T. J., Yaqoob T., Weaver K., 2007, ApJ, 670, 978

Cappi M., Tombesi F., Bianchi S., Dadina M., Giustini M., Malaguti G., Maraschi L., Palumbo G. G. C., Petrucci P. O., Ponti G., Vignali C., Yaqoob T., 2009, A&A, 504, 401

Chartas G., Brandt W. N., Gallagher S. C., 2003, ApJ, 595, 85

Chartas G., Brandt W. N., Gallagher S. C., Garmire G. P., 2002, ApJ, 579, 169

Chartas G., Saez C., Brandt W. N., Giustini M., Garmire G. P., 2009, ApJ, 706, 644

Dadina M., Cappi M., Malaguti G., Ponti G., de Rosa A., 2005, A&A, 442, 461

Elvis M., 2000, ApJ, 545, 63

George I. M., Turner T. J., Netzer H., Nandra K., Mushotzky R. F., Yaqoob T., 1998, ApJS, 114, 73

Hasinger G., 2008, A&A, 490, 905

Kaspi S., Brandt W. N., George I. M., Netzer H., Crenshaw D. M., Gabel J. R., Hamann F. W., Kaiser M. E., Koratkar A., Kraemer S. B., Kriss G. A., Mathur S., Mushotzky R. F., Nandra K., Peterson B. M., Shields J. C., Turner T. J., Zheng W., 2002, ApJ, 574, 643

King A. R., 2010a, MNRAS, 408, L95

King A. R., 2010b, MNRAS, 402, 1516

King A. R., Pounds K. A., 2003, MNRAS, 345, 657

Krolik J. H., Begelman M. C., 1988, ApJ, 329, 702

Krolik J. H., Kriss G. A., 2001, ApJ, 561, 684

Krongold Y., Nicastro F., Brickhouse N. S., Elvis M., Liedahl D. A., Mathur S., 2003, ApJ, 597, 832

Krongold Y., Nicastro F., Elvis M., Brickhouse N., Binette L., Mathur S., Jiménez-Bailón E., 2007, ApJ, 659, 1022

Krongold Y., Nicastro F., Elvis M., Brickhouse N. S., Mathur S., Zezas A., 2005, ApJ, 620, 165

Laor A., Brandt W. N., 2002, ApJ, 569, 641

Laor A., Draine B. T., 1993, ApJ, 402, 441

Liu Y., Zhang S. N., 2011, ApJ, 728, L44+

Marchesini D., Celotti A., Ferrarese L., 2004, MNRAS, 351, 733

Markowitz A., Reeves J. N., Braito V., 2006, ApJ, 646, 783

McKernan B., Yaqoob T., Reynolds C. S., 2007, MNRAS, 379, 1359

Murray N., Chiang J., Grossman S. A., Voit G. M., 1995, ApJ, 451, 498

Ogle P. M., Marshall H. L., Lee J. C., Canizares C. R., 2000, ApJ, 545, L81

Ohsuga K., Mineshige S., Mori M., Kato Y., 2009, PASJ, 61, L7+

Peterson B. M., Ferrarese L., Gilbert K. M., Kaspi S., Malkan M. A., Maoz D., Merritt D., Netzer H., Onken C. A., Pogge R. W., Vestergaard M., Wandel A., 2004, ApJ, 613, 682

Pounds K. A., King A. R., Page K. L., O'Brien P. T., 2003, MNRAS, 346, 1025

Proga D., Kallman T. R., 2004, ApJ, 616, 688

Proga D., Stone J. M., Kallman T. R., 2000, ApJ, 543, 686

Ramírez J. M., 2008, A&A, 489, 57

Ramírez J. M., 2011, RMxAA, 47, 385

Ramírez J. M., Bautista M., Kallman T., 2005, ApJ, 627, 166

Ramírez J. M., Komossa S., Burwitz V., Mathur S., 2008, ApJ, 681, 965

Reeves J. N., O'Brien P. T., Braito V., Behar E., Miller L., Turner T. J., Fabian A. C., Kaspi S., Mushotzky R., Ward M., 2009, ApJ, 701, 493

Saez C., Chartas G., Brandt W. N., 2009, ApJ, 697, 194

Saez C., & Chartas G., 2011, ApJ, 737, 91

Schurch N. J., Done C., Proga D., 2009, ApJ, 694, 1

Sim S. A., Long K. S., Miller L., Turner T. J., 2008, MNRAS, 388, 611

Sim S. A., Miller L., Long K. S., Turner T. J., Reeves J. N., 2010, MNRAS, 404, 1369

Sim S. A., Proga D., Miller L., Long K. S., Turner T. J., 2010, MNRAS, 408, 1396

Tarter C. B., Tucker W. H., Salpeter E. E., 1969, ApJ, 156, 943

Tombesi F., Cappi M., Reeves J. N., Palumbo G. G. C., Yaqoob T., Braito V., Dadina M., 2010, A&A, 521, A57+

Tombesi F., Sambruna R. M., Reeves J. N., Braito V., Ballo L., Gofford J., Cappi M., Mushotzky R. F., 2010, ApJ, 719, 700

Tombesi F., Cappi M. & Reeves J. N., 2011, arXiv:1109.2882